Tellus
SERIES A DYNAMIC METEOROLOGY AND OCEANOGRAPHY
PUBLISHED BY THE INTERNATIONAL METEOROLOGICAL INSTITUTE IN STOCKHOLM

Tellus (2008), 60A, 1038–1052
Printed in Singapore.
TELLUS

Vertical extension of the Tibetan high of the Asian summer monsoon

By T. N. KRISHNAMURTI[1*], MRINAL K. BISWAS[1] and D. V. BHASKAR RAO[2], [1]*Department of Meteorology, The Florida State University, Tallahassee, FL 32306–4520, USA;* [2]*Department of Meteorology and Oceanography, Andhra University, Visakhapatnam, India*

(Manuscript received 18 June 2007; in final form 3 July 2008)

ABSTRACT

We illustrate the vast expanse and the connection of anticyclonic flows of the Tibetan high (at the 200 hPa level) to the pole centred hemispheric North Polar anticyclone at the 10 hPa level during 1988. This feature of clockwise flows appears in the form of a tilted cone that appears to connect the Asian summer monsoon to the 10 hPa high. The anticyclonic flow tapers down to the vortex of the cone near the 400 hPa level. The tropical easterly jet of the Asian summer season is found near 10°N, at the 200 hPa level. Summer monsoon rainfall resides on the poleward side of this jet where the circulation carries a large negative relative vorticity. Over these precipitating regions, large-scale upward motion contributes to a transport of negative vorticity into the lower stratosphere. We show that this region of the stratosphere carries the kinematics for a large conversion of anticyclonic shear vorticity into anticyclonic curvature vorticity. Four-dimensional parcel trajectories emanating and rising from this region slowly carve out the hemispheric anticyclonic gyre at the 10 hPa level (i.e.) the North Polar anticyclone. This kinematics plays an important role in establishing this tilted system and a connection with the 10 hPa circulation.

1. Introduction

The northern summer stratosphere circulation shows an interesting vertical extension of the Tibetan anticyclone, from the 200 hPa level, centred near 32°N to an anticyclonic circulation centred at the North Pole at the 10 hPa level. There appears to be an inverted cone, with a tilted axis, of clockwise circulation that nearly encircles the entire Northern Hemisphere at the 10 hPa level and tapers down to a point somewhere in the Asian monsoon region near to 400 hPa level. Below that level we note the build-up of the monsoon trough that reaches to the earth's surface. Figure 1 illustrates a schematic sketch of this tilted cone. We use a red colour to show an outer closed contour of the North Polar anticyclone and the blue colours to show the vertical structure of the monsoon trough. This cone connects the summer monsoon circulations of Asia with the stratospheric circulation. In this illustration we note the climatological expanse of the clockwise flows of the cone. Below this cone, lies the cyclonic circulation of the monsoon trough in the lower troposphere, which is also displayed here. This short paper illustrates a connection of the active monsoon trough of the lower troposphere with the North Polar anticyclone of the stratosphere during 1988, a feature that can be seen over most years during the summer season. The year 1988 was selected because it was a heavy monsoon rainfall year. During the years 1982–1992 the annual all India summer monsoon rainfall was 735.6, 955.6, 836.9, 760.0, 743.2, 697.4, 961.7, 866.9, 908.8, 784.7 and 785.0 mm, respectively (Parthasarathy et al., 1995). The North Polar anticyclone and the vertical structure of the monsoon trough seem to be clearly connected, the Tibetan anticyclone at 200 hPa was always recognized as a part of the monsoon complex and its ties to the monsoon trough have been discussed by many authors, for example, Rao (1976) and Krishnamurti and Bhalme (1976). The upper reaches of the Tibetan anticyclone were also known to climatologists, Hastenrath (1991). The importance of shear to curvature kinematics of the wind field, especially above the 300 hPa level is a new aspect that ties the troposphere and the stratosphere. We are not describing a simple hydrostatic thermal coupling of different layers. This is hard to visualize as a single vertically coupled static system since it exhibits such a large tilt (i.e. from 35°N at the 200 hPa to the North Pole at the 10 hPa level). The connecting link between the troposphere and stratosphere is not a simple (out of phase) hydrostatic vertical structure. Looking at a sequence of maps at vertical intervals of 50 hPa one can see this continuity and the link of these systems. That link, we portray here, arises from two kinematic considerations, the upward flux of anticyclonic vorticity associated in the active precipitating monsoon regions and a

*Corresponding author.
e-mail: tnk@io.met.fsu.edu
DOI: 10.1111/j.1600-0870.2008.00359.x

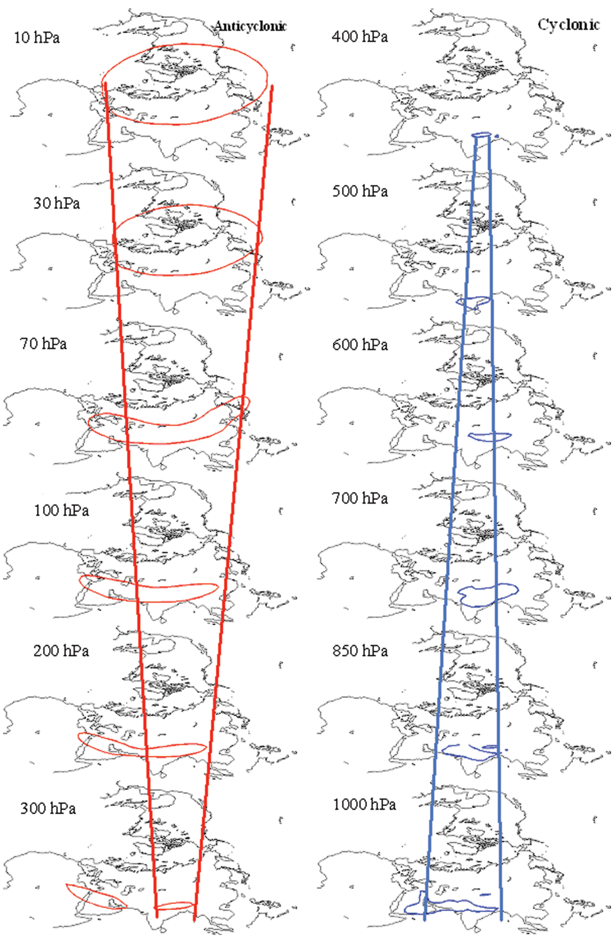

Fig. 1. Schematic picture of the cone, showing the shape of the anticyclonic flows at different levels from 1000 to 10 hPa levels and cyclonic flows down to the surface.

rapid conversion (and its expanse) from anticyclonic shear to the anticyclonic curvature vorticity. We normally speak of large tilts in baroclinic systems where an upper anticyclone may overlie a surface cyclone. Our study suggests that the large vertical tilt of the Tibetan anticyclone arises here from a combination of factors such as the vertical advection of negative relative vorticity in the summer stratospheric fountain and the flow kinematics.

In this paper, we illustrate the vertical mass flux and the flux of negative relative vorticity from the troposphere to the stratosphere over the Asian monsoon region during 1988. Most of the summer monsoon precipitation is found north of the tropical easterly jet (which is located near 10°N and 175 hPa level). This region north of 10°N carries large negative vorticity (anticyclone shear as well as curvature). We furthermore show that, as this negative vorticity is being advected upward from the troposphere to the lower stratosphere and the shear vorticity is continually being transformed into curvature vorticity of anticyclonic flows in the lower stratosphere. That feature contributes to a slow growth of a sweep of anticyclonic curvature over the stratosphere resulting in the flow encircling the North Pole and in the establishment of the North Polar anticyclone at to the 10 hPa level. In shear flow dynamics the conversion of anticyclonic shear into anticyclonic curvature can arise from barotropic dynamics. This can be an effective process if a steady generation of anticyclonic shear in upper tropospheric diverging flows is present. The conversion to curvature vorticity depends on a number of kinematic flow parameters such as the increase or decrease of wind speed along the flow, the rate of change of the angle the flow field makes with respect to the latitude circle and the orientation of the geopotential field with respect to the flow field. We shall be illustrating these factors in the evolution of anticyclonic flows of the Northern Hemisphere during the summer season.

1.1. The stratospheric fountain of northern summer

Newell and Gould-Stewart (1981) coined the word 'The Stratospheric Fountain' for the upward flux of mass from the troposphere to the lower stratosphere. The tall cumulonimbus clouds of the winter monsoon near Borneo and Indonesia often exhibit overshooting of upward mass flux above these clouds. Here a cold stratosphere with temperatures near −80 °C is maintained by adiabatic cooling of the rising air and the evaporation of cloud hydrometeors. Danielsen (1993) studied this region, over the winter monsoon, utilizing a NASA (acronyms are listed in Table 1) ER2 aircraft that could fly at levels as high as 19 500 m. Danielsen concluded that this region of strong vertical mass flux (the stratospheric fountain) carries a substantial moisture transport from the troposphere to the lower stratosphere contributing to the possible maintenance of the moisture balance of the lower stratosphere. A northern summer stratospheric fountain has also been mentioned in literature, (Atticks and Robinson, 1983; Frederick and Douglass, 1983; Mote et al., 1996). The most active longitude of the northern summer stratospheric fountain seems to lie between 95°E and 110°E over the eastern foothills of the Himalayas where the precipitation is more. A north–south vertical cross-section from roughly 20°N to the northern pole, along these longitudes (not shown) provides interesting information on the shape of this stratospheric fountain.

1.2. Tropical easterly jet

This well known tropical easterly jet stream (Koteswaram, 1958; Chen, 2005) is a major component of the Asian summer monsoon circulation. Its average intensity is approximately 24 m s^{-1} and peaks to 35 m s^{-1} resides near 10°N at the 175 hPa level extending from Bay of Bengal over to the Arabian sea and the African coast. Figure 2 illustrates a view of the jet for the month of August 1988. This jet emanates from the anticyclonic circulation of the Tibetan anticyclone. The illustration shows the isotachs and streamlines at the 200 hPa level and the surface precipitation amounts (superimposed) for August 1988 in mm d^{-1}. It is worth noting that most of the monsoonal precipitation

Table 1. Acronyms and symbols

Acronym/symbol	Description
u	Zonal wind
v	Meridional wind
V	Scalar wind $(u^2 + v^2)^{1/2}$
w	Vertical z-velocity
ω	Vertical p-velocity
f	Coriolis parameter
g	Acceleration due to gravity
s	Axis along the motion
n	Axis normal to the motion
t	Time coordinate
p	Pressure
θ	Potential temperature
ζ	Relative vorticity
ζ_a	Absolute vorticity
a	Rotation angle subtended with respect to x-axis
φ	Geopotential
S	Shear vorticity
S_t	Stability
C	Curvature vorticity
E	Earth's vorticity
PV	Potential vorticity
ECMWF	European Centre for Medium-Range Weather Forecasts
NCAR	National Center for Atmospheric Research
NCEP	National Centers for Environmental Prediction
NASA	National Aeronautics and Space Administration
ERA-40	ECMWF Re-Analysis
QBO	Quasi-Biennial Oscillation
TBO	Tropospheric Biennial Oscillation
EP	Eliassen-Palm
TEJ	Tropical Easterly Jet

resides on the anticyclonic shear side of this jet where the curvature of flow is also anticyclonic. Thus any upward motion ($\omega < 0$) in the broad rainy regions contributes to an upward flux of negative relative vorticity from the troposphere to the lower stratosphere. That is an important aspect of this study.

2. Data and methodology

The data used for the computations and analyses of this study are taken from the ERA-40 and NCEP/NCAR (Kalnay et al., 1996) reanalysis fields. The European Centre for Medium Range Forecasting (ECMWF) provides 40-yr (ERA-40) reanalysis fields for the period September 1957 to August 2002 (http://www.ecmwf.int/research/era/). ERA-40 is a second generation reanalysis product following the ERA-15 (Gibson et al., 1997). ERA-40 is used mostly for computations of different quantities unless otherwise stated.

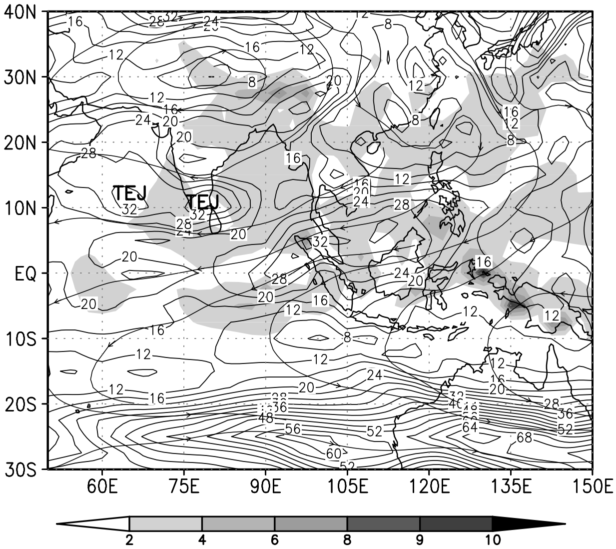

Fig. 2. Isotachs (solid lines drawn at intervals of 4 m s^{-1}) and streamlines (thin lines) of the wind flow at 200 hPa level August 1988. Precipitation (mm d^{-1}) for August 1988 is shown as grey shading. TEJ is Tropical Easterly Jet.

2.1. *Transformation of shear to curvature vorticity*

The anticyclonic vorticity that is being vertically advected by the monsoon seems to be steadily converted to anticyclonic curvature vorticity. That is an important aspect of the kinematics and dynamics of the exchange of air from the troposphere to the lower stratosphere over this region. The conservation of absolute vorticity, (following a parcel) carries within it, mutual exchange of vorticity among its components (i.e.) shear (S), curvature (C) and the earth's vorticity (E). Following Bell and Keyser (1993), the vertical component of relative vorticity can be defined as the sum of $(-\frac{\partial V}{\partial n})$ and $\left(V\frac{\partial \alpha}{\partial s}\right)$ which corresponds to shear and curvature vorticity, respectively, in natural coordinate system. One can schematically write this as:

$$\frac{dC}{dt} = \langle S \cdot C \rangle + \langle E \cdot C \rangle$$

$$\frac{dS}{dt} = -\langle S \cdot C \rangle + \langle E \cdot S \rangle$$

$$\frac{dE}{dt} = -\langle E \cdot C \rangle - \langle E \cdot S \rangle .$$

The symbol for the vorticity exchange function $\langle AB \rangle$ denotes an exchange of vorticity from the first member A to the second member B.

Note that

$$\frac{d\zeta_a}{dt} = \frac{d}{dt}(C + S + f) = 0$$

for conservation of absolute vorticity.

This topic has been discussed in literature by several authors including Bell and Keyser (1993) and Viudez and Haney (1996). Our interest in this problem is on the large generation of anticyclonic curvature vorticity during the Northern Hemisphere summer over the stratosphere. Thus we shall only be highlighting the function $\langle S \cdot C \rangle$ and its mapping over the stratosphere. Following Bell and Keyser (1993), we denote $\langle S \cdot C \rangle$ by the function

$$\langle S \cdot C \rangle = -\left(\frac{\partial V}{\partial s}\right)\left(\frac{\mathrm{d}\alpha}{\mathrm{d}t}\right) - \frac{\partial}{\partial n}\left(\frac{\partial \varphi}{\partial s}\right). \quad (1)$$

This expression is in the natural coordinates. The variables V and φ denote scalar wind and geopotential, respectively and α denotes the angle subtended by the velocity vector with respect to the x-axis (positive when the orientation is anticlockwise). We do not include the Coriolis since we are only addressing the shear to curvature exchanges of relative vorticity.

Bell and Keyser (1993) also provide a convenient computational form for $\langle SC \rangle$ in the Cartesian coordinates where the conversion terms are expressed by:

$$\frac{\partial V}{\partial s} = \frac{1}{V^2}\left[\left(u^2 u_x + v^2 v_y\right) + uv(v_x + u_y)\right] \quad (2)$$

$$\frac{\mathrm{d}\alpha}{\mathrm{d}t} = \frac{1}{V^2}(v\varphi_x - u\varphi_y) \quad (3)$$

$$\begin{aligned}\frac{\partial}{\partial n}\left(\frac{\partial \varphi}{\partial s}\right) = {} & \frac{1}{V^2}\left[(u^2 - v^2)\varphi_{xy} - uv(\varphi_{xx} - \varphi_{yy})\right] \\ & + \frac{uv}{V^4}\left[(v_x + u_y)(v\varphi_x - u\varphi_y) + vu_x\varphi_y - uv_y\varphi_x\right] \\ & + \frac{1}{V^4}\left(u^3 v_y \varphi_y - v^3 u_x \varphi_x\right). \quad (4)\end{aligned}$$

The variables u and v denote zonal and meridional components of the wind and subscripts indicate partial differentiation. In eqs(3) and (4), partial differentiation in the Cartesian coordinate system is denoted using subscripts. Given the wind components and the geopotential data sets at synoptic time intervals, it is possible to compute and map the function $\langle S \cdot C \rangle$ over any desired region. This map conveys to us regions where cyclonic (>0) or anticyclonic (<0) curvature vorticity is being generated from the prevailing shear vorticity. Given the large vertical (upward) transport of negative relative vorticity from the monsoon region, this paper illustrates the conversion process that generates large amounts of anticyclonic curvature vorticity over most of the lower stratosphere

3. Results

In this section, the results of computations are presented.

3.1. *Onsets of Myanmar/South China Sea/Indian monsoon and evolution of stratospheric clockwise circulation*

A major transition to a global clockwise circulation centred at the North Pole at the 10 hPa level occurs annually in the late spring and early summer months. This transition seems to coincide with the months of onset of summer monsoon rains over Myanmar/South China Sea and India. The Myanmar/South China Sea onset occurs in early May generally, whereas the Indian monsoon follows during early June. The polar circulations in April generally carry a low pressure at the 10 hPa level (Fig. 3). As we proceed from early April to the middle of May, the 10 hPa circulation transitions to clockwise flows around almost the entire Northern Hemisphere. That kind of spectacular change of stratospheric circulation is an annual event and the transitions are shown in Fig. 3. It is suggestive that as the monsoon evolves, so does the stratospheric clockwise gyre around the North Pole, especially at the 10 hPa level.

3.2. *Stratospheric anticyclone*

The upward growth of anticyclonic circulation can be seen clearly from the closed contours of the anticyclone at several successive pressure levels of the reanalysis field. Those at 300, 200, 150, 100, 50, 40, 30 and 10 hPa levels are illustrated in Figs. 4 and 5. Figure 4 shows the anticyclonic circulation for the month of August 1988 and Fig. 5 shows the mean for the years 1984–2002 for the same month. The Tibetan anticyclone can be seen at the 300 hPa level and has a crescent shape. That shape amplifies and becomes more circular as we proceed up to the 150 hPa level. It appears that anticyclonic curvature vorticity gets spread around the Northern Hemisphere as we proceed upwards from the 150 hPa level. The anticyclonic closed contours reach all around the Northern Hemisphere by around 40 hPa level. The signature of the Tibetan high is slowly replaced between 40 and 10 hPa levels into a hemispheric polar anticyclone centred at the North Pole.

3.3. *Vertical spread of anticyclonic vorticity*

As we proceed up from the 300 hPa level to the 10 hPa level, we can see a spread of anticyclonic vorticity that encircles the North Pole (Fig. 6 for August 1998). This ring of anticyclonic vorticity almost encircles the latitude circles (roughly between 20°N and 40°N) by the 100 hPa level. The global extent of this feature is most prominent above the 100 hPa level where we see the spread of anticyclonic vorticity over the hemisphere at the 10 hPa level. The largest values of the anticyclonic vorticity reside between the 100 and 200 hPa levels. The maximum values of the anticyclonic vorticity are around -1×10^{-5} s^{-1} at the 10 hPa level whereas they carry values as high as -2×10^{-5} s^{-1} at the 100 hPa level. We shall next illustrate the:

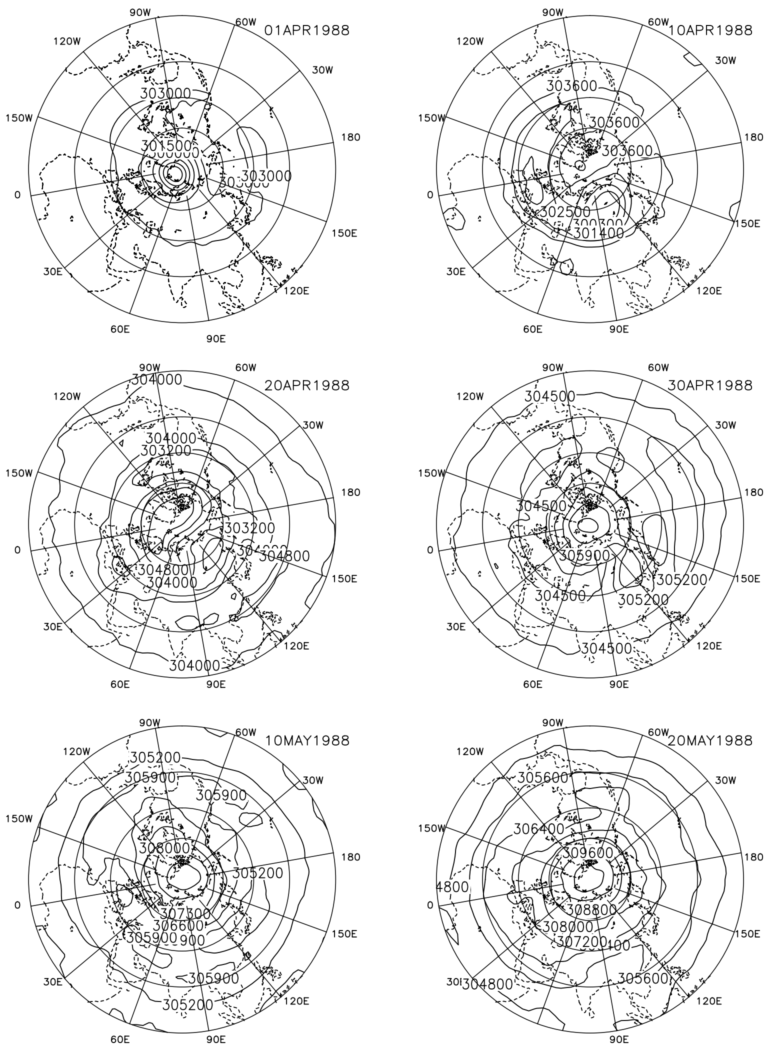

Fig. 3. Time history of geopotential ($m^2\ s^{-2}$) at 10 hPa from 1 April 1988 up to 20 May 1988.

(i) The monsoonal anticyclonic curvature, and shear.

(ii) The upward flux of the anticyclonic vorticity.

(iii) A large continual conversion of this shear vorticity to the anticyclonic curvature vorticity in the lower stratosphere.

Figure 7a illustrates the zonal curvature averaged between 20°N and 40°N latitudes, respectively. Figure 7b illustrates the shear vorticity zonally averaged between 20°N and 40°N, respectively (negative values denote anticyclonic vorticity). Here we note vertical extensions of these tubes all the way to the 30 hPa level and even higher. These are daily zonal averages averaged between 20°N and 40°N for an entire monsoon season. (We did not show regions of cyclonic vorticity deliberately to emphasize the horizontal spread of the anticyclonic shear and curvature). In Fig. 7c, the upward flux of anticyclonic vorticity is shown. This shows an upward flux of anticyclonic vorticity up to 30 hPa and beyond. In Fig. 8, we see a preponderance of the exchange of shear to curvature vorticity in generating anticyclonic vorticity. This feature also extends up from the Tibetan Plateau all the way to the 30 hPa level and above, illustrated later in the text. We interpret this to imply that the entire lower stratosphere experiences a large generation of anticyclonic curvature vorticity from the kinematics of the motion field. The monsoonal heavy rains and rising motion occur in regions of large upper tropospheric anticyclonic vorticity. We have shown a steady upward flux of this vorticity into the lower stratosphere where this rich kinematic property of flows was noted to prevail. This enriches the anticyclonic flow over the hemisphere and contributes to the maintenance of the North Polar anticyclone.

3.4. Vertical motions

In Fig. 9, we display fields of mean vertical motion 'ω' over the Northern Hemisphere for the month of August 1988. These fields cover the geographical distribution of the vertical motions at 300, 200, 100, 50, 30 and the 10 hPa levels. A simple colour

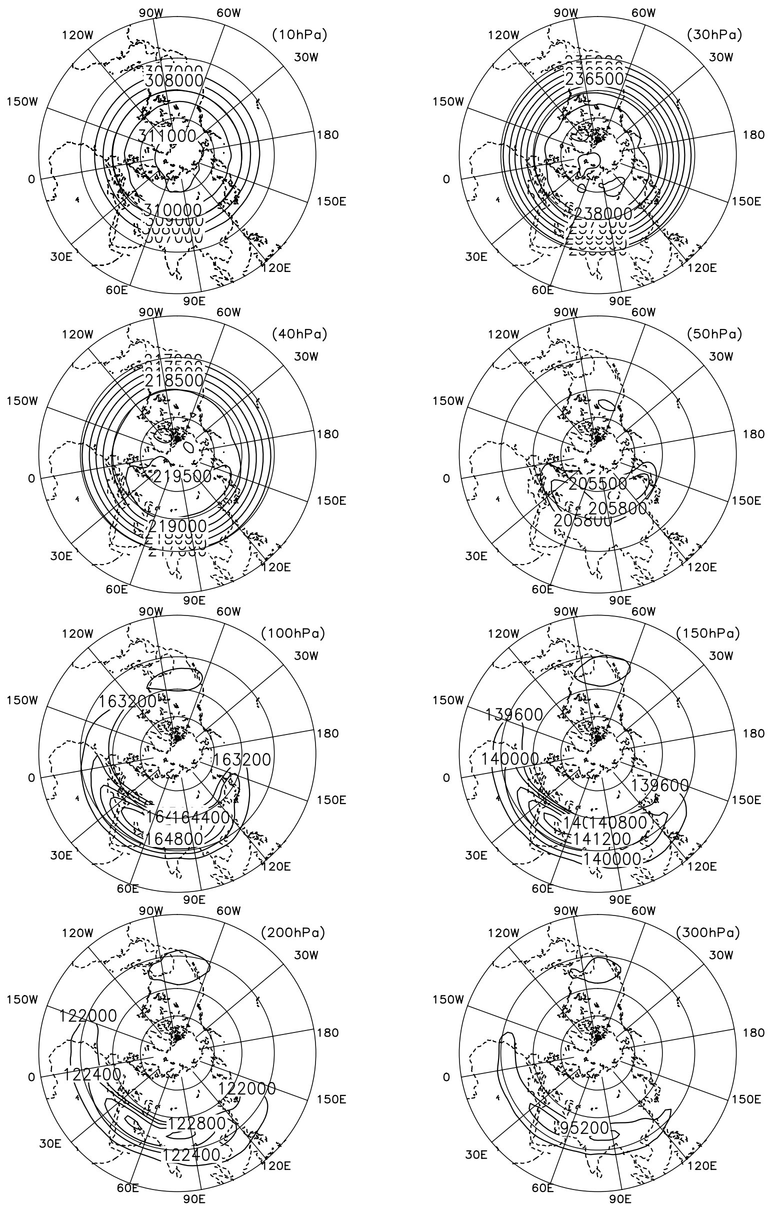

Fig. 4. Geopotential ($m^2\ s^{-2}$) at different vertical levels from 300 to 10 hPa computed as mean for August 1988.

scheme displays red for rising and blue for sinking motion. The most relevant features for this study are the rising lobes of air over the Asian summer monsoon that seems to cover a large area with the largest magnitudes residing over the eastern foothills of the Himalayas. Those magnitudes are as high as 150 Pa h^{-1} at the 300 hPa level. The rising lobes of air at the 50 hPa level over the monsoon region carry the anticyclonic vorticity (north of the easterly jet) into the lower stratosphere. It should be noted that these vertical motions are a part of the ERA-40 reanalysis.

3.5. Vertical transport of vorticity

A mapping of the product of vertical velocity ω and the relative vorticity ζ at several vertical levels shows regions where anticyclonic vorticity is being transported from the troposphere to the stratosphere. A positive value for this product, in the region of upward motion, implies an upward flux of anticyclonic relative vorticity at that location. In Fig. 10, we show these fields at the 300, 200, 100, 50, 30 and 10 hPa levels. We note that substantial areas (where $\omega < 0$) carry a positive sign implying that anticyclonic relative vorticity is being transported into the stratosphere. These transports are largest near the 200 and 100 hPa levels over the regions of the Asian monsoon. Furthermore, we note a falling off of the magnitude of these upward fluxes as we move to 50, 30 and 10 hPa levels. That implies a large convergence of vertical flux of anticyclonic vorticity at these levels especially over the monsoon region.

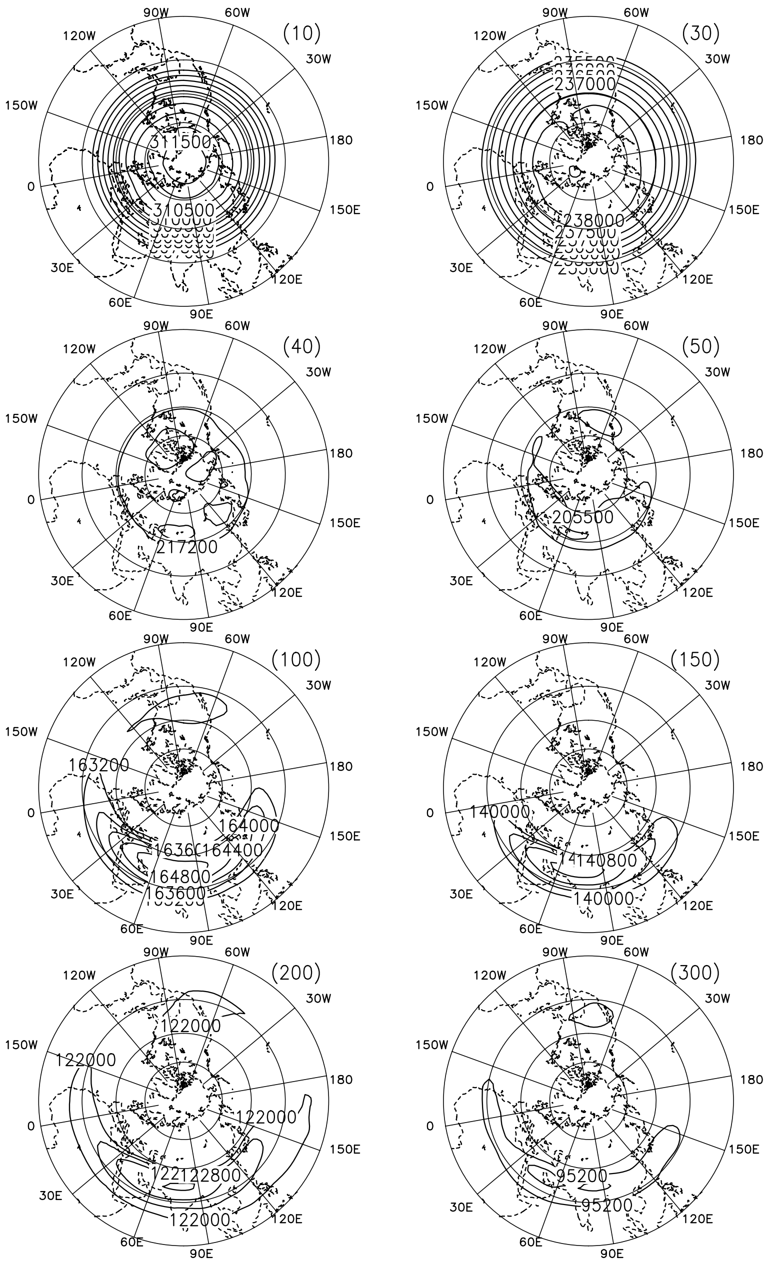

Fig. 5. Same as in Fig. 4 except averaged between August 1984 and 2002. Coastline is shown as broken and contours are shown as solid lines. Only the contours relevant to the identification of the cone are shown.

3.6. Conversion from shear to curvature vorticity

The kinematics of the conversion of shear to curvature vorticity can be interpreted from an examination of the expression given by eq. (1). Because the expression is in natural coordinates it is difficult to provide a simple physical interpretation for $\langle S \cdot C \rangle > 0$ (see Bell and Keyser, 1993). However, we note the following scenarios.

The increase (decrease) of speed along the trajectory is given by $\frac{\partial V}{\partial s} > (<) \, 0$ respectively. The direction of flow with respect to the latitude circle, defined by the angle α, can increase or decrease following the parcel motion (i.e.) $\frac{\mathrm{d}\alpha}{\mathrm{d}t} > (<) \, 0$, respectively. $\frac{\mathrm{d}\alpha}{\mathrm{d}t} > 0$ implies that the angle between the parcel trajectory and the latitude circle is increasing, if at the same time parcels move towards stronger velocity V, that is, $\frac{\partial V}{\partial s} > 0$ then the anticyclonic curvature of the parcel would increase. There are several possibilities here (if we assume the right-hand side of eq. 1 to be zero):

(i) $\frac{\partial V}{\partial s} > 0$; $\frac{\mathrm{d}\alpha}{\mathrm{d}t} > 0$ hence $\langle SC \rangle < 0$
(ii) $\frac{\partial V}{\partial s} < 0$; $\frac{\mathrm{d}\alpha}{\mathrm{d}t} < 0$ hence $\langle SC \rangle < 0$
(iii) $\frac{\partial V}{\partial s} < 0$; $\frac{\mathrm{d}\alpha}{\mathrm{d}t} > 0$ hence $\langle SC \rangle > 0$
(iv) $\frac{\partial V}{\partial s} > 0$; $\frac{\mathrm{d}\alpha}{\mathrm{d}t} < 0$ hence $\langle SC \rangle > 0$.

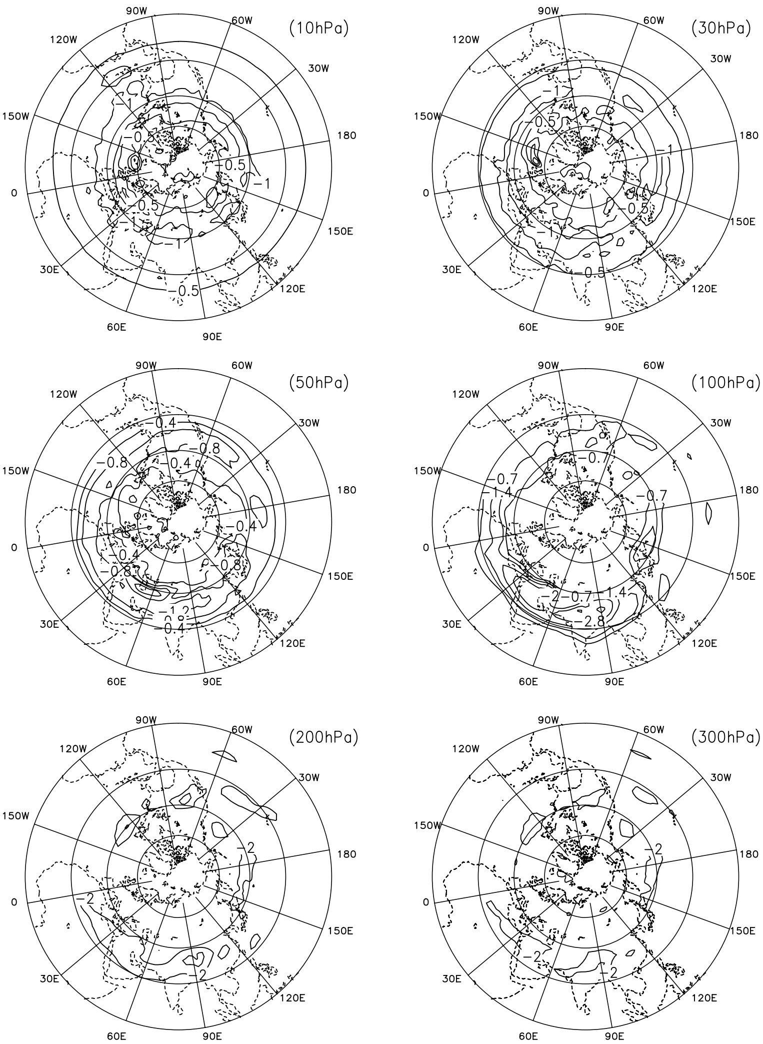

Fig. 6. Same as of Fig. 4 but for relative vorticity (10^{-5} s^{-1}) for August 1988.

In order for shear vorticity to transform into (anticyclonic) curvature vorticity, we need a negative contribution from the terms on the right-hand side of eq. (1), that means a positive contribution for the product of $\frac{\partial V}{\partial s}$ and $\frac{d\alpha}{dt}$ (due to the negative sign attached). Similarly the second term of the shear vorticity to curvature vorticity require that $-\frac{\partial}{\partial n}\frac{\partial \varphi}{\partial s}$ be < 0. That will happen if the cross flow gradient of $\frac{\partial \phi}{\partial s}$ of the along flow gradient of geopotential is positive, this simply implies that the geopotential gradients along the flow increases across the direction of flow leading to an enhancement of anticyclonic curvature.

The dynamical implication of $\langle S \cdot C \rangle$ is essentially a barotropic concept. What we find is a continual large upward transport of negative shear vorticity (which abounds north of the tropical easterly jet); that shear vorticity sees a continual transportation into anticyclonic curvature vorticity at the upper level as a consequence of the prevailing kinematics of the motion field.

We noted that each of the terms on the right-hand side of eq. (1) were negative, they contributed to $\frac{dC}{dt} < 0$ over most regions north of 25°N.

If we select a number of parcel trajectories that originate over the heavy rain belt of the eastern foothills of the Himalayas, we can calculate these respective terms along the trajectory (following their Cartesian representation described in eqs 2–4). That part of the kinematics is presented in Table 2. The entries in the table carry the following information for various parcels: latitude, longitude, pressure level, $\frac{\partial V}{\partial s}$, $\frac{d\alpha}{dt}$ and $\frac{\partial}{\partial n}\left(\frac{\partial \varphi}{\partial s}\right)$. These are daily values for 8 August 1988. In Table 2 we provide entries for the rate of change of shear 'S', that is, $\frac{dS}{dt} = \frac{\partial V}{\partial s}\frac{d\alpha}{dt} + \frac{\partial}{\partial n}\frac{\partial \varphi}{\partial s}$. These two terms on the right-hand side are positive and so is their sum 'S' to begin was <0 (anticyclonic shear). The positive value of $\frac{dS}{dt}$ implies that 'S' should carry reduced anticyclonic shear after a time Δt, this result in an increase of anticyclonic curvature 'C' as we proceed in time. The positive values on the last column of Table 2 implies an increase of anticyclonic curvature with time.

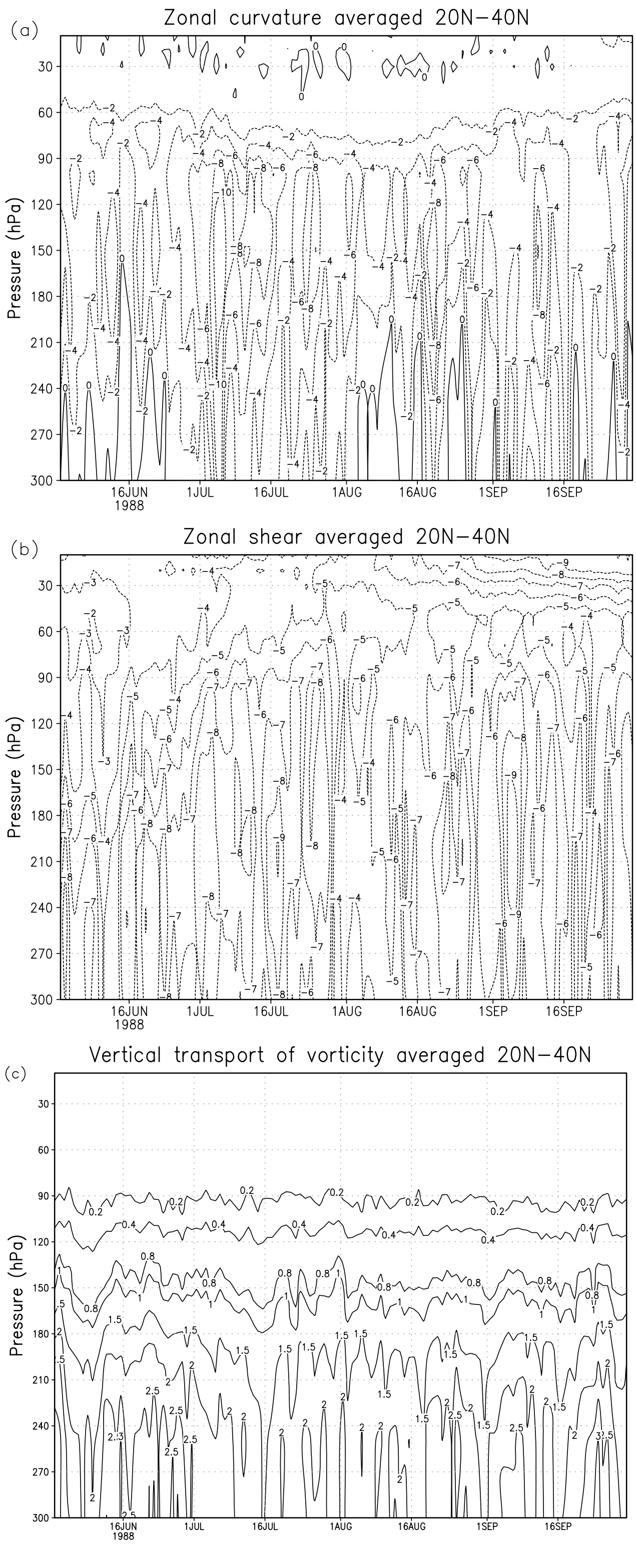

Fig. 7. Vertical reach of monsoonal (a) anticyclonic curvature (10^{-06} s^{-1}) zonal averaged between 20°N and 40°N. (b) Anticyclonic shear (10^{-06} s^{-1}) zonal averaged between 20°N and 40°N. (c) Anticyclonic vorticity (10^{-06} s^{-1}) zonal averaged between 20°N and 40°N.

This table only includes a very small subset of data for $\langle S \cdot C \rangle$. In order to portray the geographical spread of $\langle S \cdot C \rangle$ over the upper troposphere and lower stratosphere, we have mapped $\langle S \cdot C \rangle$ over the pressure levels 300, 200, 100, 50, 30 and 10 hPa (Fig. 11). We note here a very large preponderance of negative values (increase of anticyclonic curvature) over the entire hemisphere. In the Northern Hemisphere summer, the kinematics of flows in the lower stratosphere prefers an exchange of

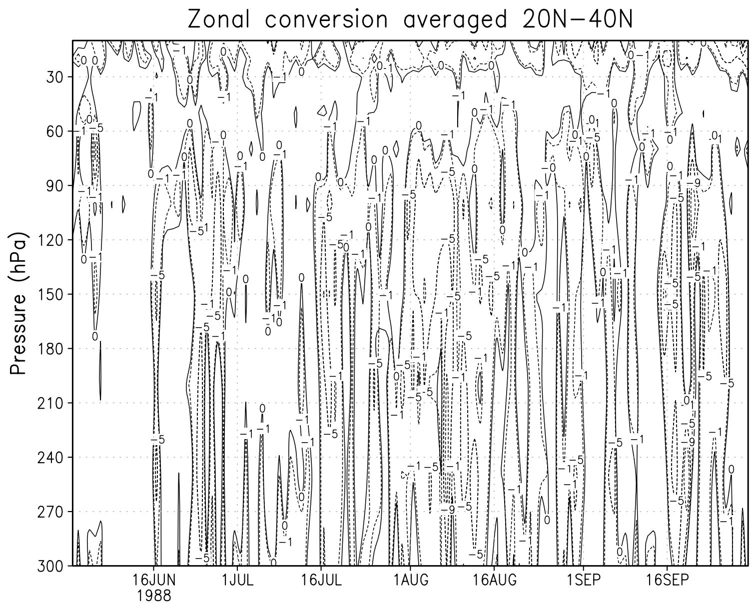

Fig. 8. Vertical reach of monsoonal conversion of shear to curvature vorticity (10^{-12} s^{-2}) zonally averaged between 20°N and 40°N.

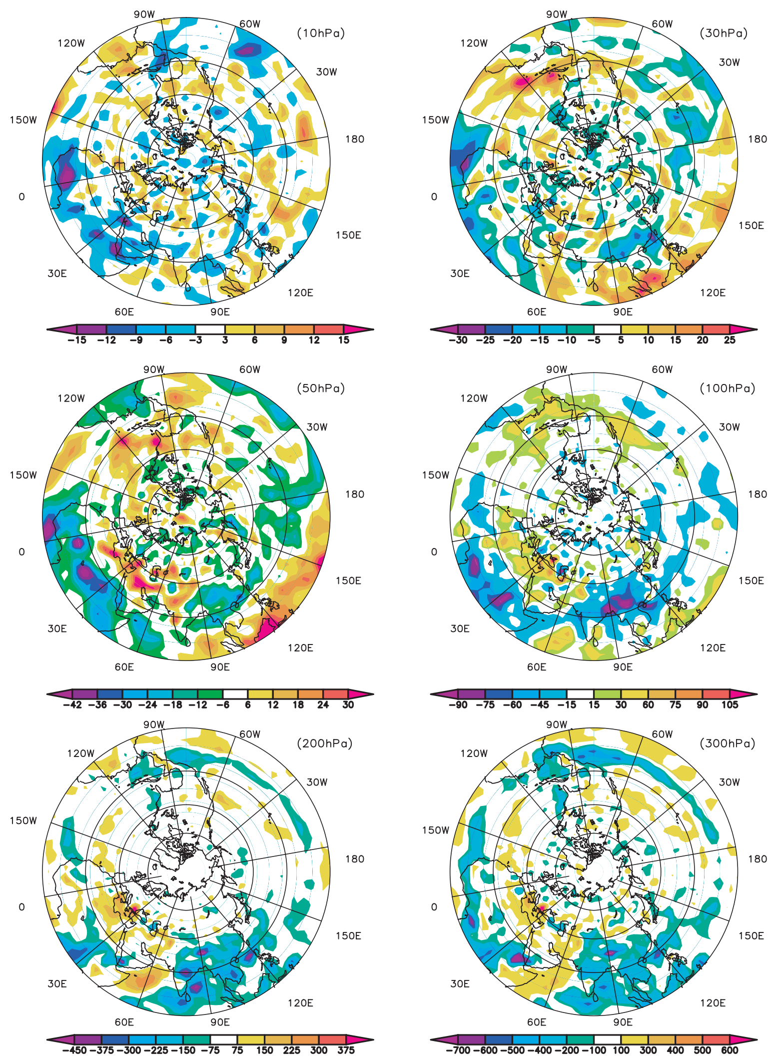

Fig. 9. Vertical motion field (Pa h^{-1}) at different vertical levels from 300 to 10 hPa computed as mean for August 1988. Coastline is shown as solid line. Positive (downward motion) values are shown as blue contours and negative (upward motion) values are shown as red contours.

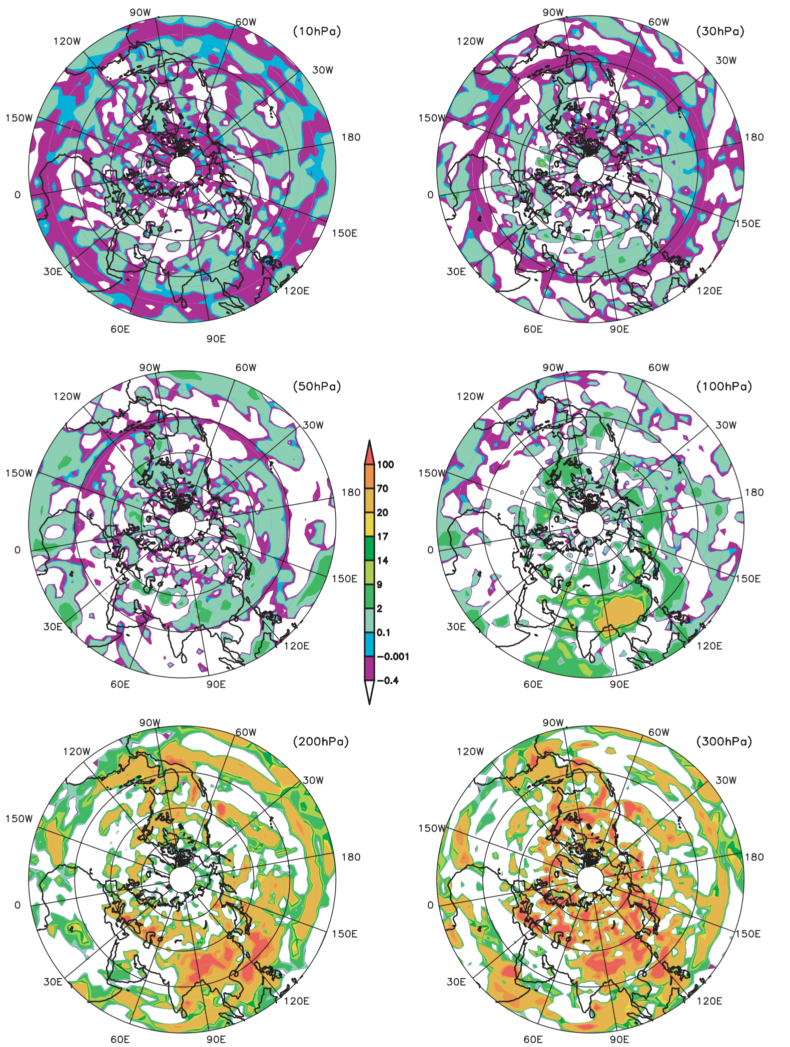

Fig. 10. Vertical advection of relative vorticity (10^{-08} Pa s^{-2}) at different vertical levels from 300 to 10 hPa computed as mean for August 1988. Coastline is shown as solid line.

Table 2. The magnitudes of different terms of the shear to curvature vorticity computed for 8 August 1988

Numbers	Lat. (°N)	Lon. (°E)	Lev. (hPa)	$\frac{\partial V}{\partial s}$ (s^{-1}) (10^{-06})	$\frac{d\alpha}{dt}$ (s^{-1}) (10^{-05})	$\left(\frac{\partial V}{\partial s}\right)\left(\frac{d\alpha}{dt}\right)$ (s^{-2}) (10^{-11})	$\frac{\partial}{\partial n}\left(\frac{\partial \varphi}{\partial s}\right)$ (s^{-2}) (10^{-11})	Total (s^{-2}) (10^{-10})
1	32.5	92.5	200	1.003	0.366	0.3679	0.442	0.081
2	35.0	100	100	13.22	0.8319	11	0.551	11.55
3	42.5	82.5	50	−3.37	−2.81	9.5	13.66	2.31
4	47.5	105	30	0.1926	0.9119	0.175	1.03	0.12
5	32.5	102.5	10	4.24	0.913	3.88	9.77	1.366

vorticity from shear to anticyclonic curvature. The largest values of this exchange are seen over the East Asian monsoon at the 100 and 200 hPa level. Thus it appears that parcels of air ascending over the general region of the summer monsoon convey negative relative vorticity into a region where kinematics of shear to curvature transform most of it to anticyclonic curvature vorticity that eventually sweep encircles the North Pole. This can further be illustrated from four directional trajectories.

3.7. *Trajectories*

Trajectories are used to trace parcel motion in four-dimensions. From these calculations, it is possible to obtain the origin of a parcel of air that has a certain property or tracer component based on the principle that the displacement of the parcel of air will be produced by the components of the three-dimensional wind field (Krishnamurti and Bounoua, 1996). Horizontal and vertical

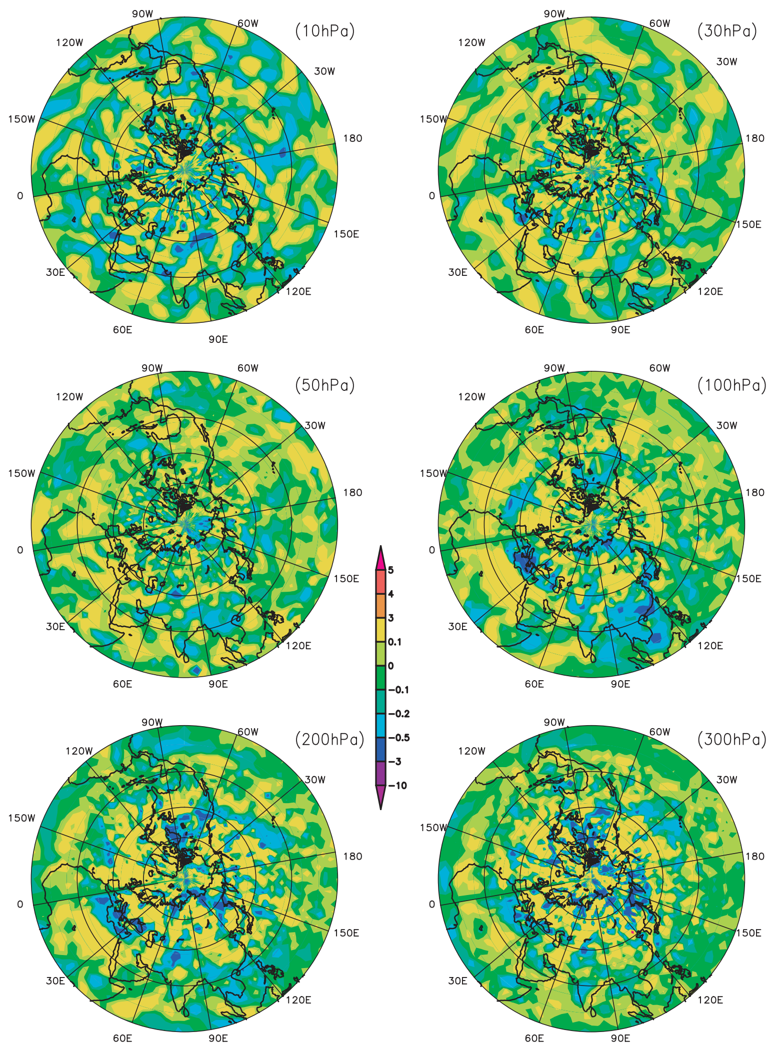

Fig. 11. Conversion form shear to curvature vorticity (10^{-10} s^{-2}) at different vertical levels from 300 to 10 hPa computed as mean for August 1988. Coastline is shown as solid line.

displacements, D_x, D_y and D_p, at any point along the trajectory for a short period of time are calculated using Newton's Law, and can be described as:

$$\begin{aligned} D_x &= uD_t + 0.5(a_x)D_{tt} \\ &= 0.5\{u + [u + (a_x)D_t]\}D_t \\ &= 0.5(u + u')D_t \end{aligned} \tag{5}$$

$$\begin{aligned} D_y &= v\ Dt + 0.5(a_y)D_{tt} \\ &= 0.5\{v + [v + (a_y)D_t]\}D_t \\ &= 0.5(v + v')D_t \end{aligned} \tag{6}$$

$$\begin{aligned} D_p &= wD_t + 0.5(a_p)D_{tt} \\ &= 0.5\{w + [w + (a_p)D_t]\}D_t \\ &= 0.5(w + w')D_t. \end{aligned} \tag{7}$$

(where the subscripts indicate differentiation)where a_x, a_y and a_p are the parcel's acceleration along the horizontal and vertical axes. The prime terms u', v' and w' are the velocity components at the end of the trajectory (Krishnamurti and Bounoua, 1996). Initially, displacements are computed without acceleration. The end point wind components are interpolated and used in eqs (1)–(3); iteration of the equations improves the values of u', v' and w'. The next point is calculated from the starting point by the displacement in the horizontal and vertical direction, D_x, D_y and D_p. This is a well known procedure for semi-Lagrangian computations.

When we constructed a number of four-dimensional trajectories using the above methodology, we found that: (i) Parcels originating near the 200 hPa surface over the heavy rainfall region (eastern foothills of the Himalayas) showed a clockwise circuit around the Tibetan high and soon leaving this feature and making a clockwise circuit around the North Pole. (ii) The magnitudes of the vertical motions were roughly of the order of 100 hPa/50 d, so these parcels only rose to roughly the 100 hPa level. (iii) We successively constructed forward trajectories originating near the 200, 100, 50 and 30 hPa levels. These trajectories

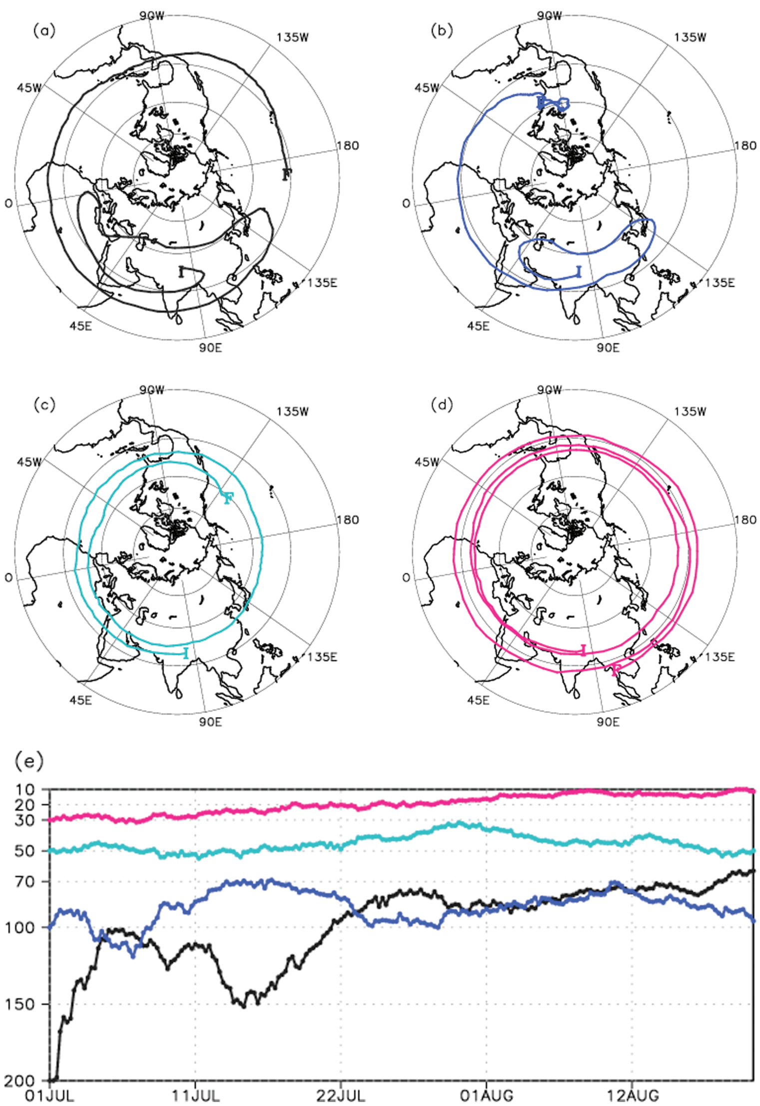

Fig. 12. Parcel trajectories for the duration of 50 d starting on 1 July 1988 with origination at the levels (a) 200 hPa (b) 100 hPa (c) 50 hPa and (d) 30 hPa. I denotes the origination point and F denotes the finishing point. Panels (a)–(d) show the horizontal displacement of the four individual parcels and panel (e) shows the vertical displacement of all the four parcels depicted in (a)–(d).

covering a 50 d span are illustrated in Figs. 12(a–d). (iv) The behaviour of the trajectories at the 100 hPa level again reflected a circuit around the Tibetan high prior to its pathway around the North Pole. (v) The parcels originating from the monsoon region over the eastern Himalayas at 50 and 30 hPa levels both exhibited clockwise, around the pole circuits. The zonal motions at the 30 hPa were clearly somewhat faster than those at the 50 hPa level. (vi) The higher levels to which these parcels arrive at are illustrated in Fig. 12(e). The most dramatic rise is for the parcels at the 200 hPa level that make it to near the 100 hPa level in 45 d. Parcels originating at these other levels show successively lesser ascent rates. It is interesting to note that parcels that were launched at the 30 hPa made it to the 10 hPa during this time interval, making no less than three circuits around the globe. The interpolated values of $\langle S \cdot C \rangle$ were plotted along the trajectories and we noted nearly all along the trajectory a conversion to anticyclonic curvature.

If we consider the entire vertical column above the heavy monsoon rainfall region (between 200 and the 30 hPa levels), these parcels provide the best link between the Tibetan high and the North Polar anticyclone. Successively, parcels seem to overshoot the tropopause (near 150 hPa level) and a collection of them carve out the major northern summer anticyclone of the polar circulation even up to the 10 hPa level. The kinematics along the pathways of these trajectories strongly favours a transport of the shear vorticity into the anticyclonic curvature vorticity. These kinematics facilitate the evolution of the clockwise circulation around the North Pole during the northern summer season.

4. Discussion

This paper emphasizes the generations of anticyclonic curvature vorticity over the upper troposphere and the lower stratosphere during the monsoon months. It should be noted that this kinematic argument is equally applicable to the conversion of potential vorticity (PV). In that framework one needs to simply multiply the components of vorticity by a static stability term $-g\frac{\partial\theta}{\partial p}$ at each location. Given the relation for the conservation of PV,

$$\frac{\mathrm{d}}{\mathrm{d}t}PV = 0$$

or $\frac{\mathrm{d}}{\mathrm{d}t}(S_t \cdot \varsigma_{a\theta}) = 0$, where S_t is the static stability

$$\text{or } S_t\frac{\mathrm{d}\varsigma_{a\theta}}{\mathrm{d}t} + \varsigma_{a\theta}\frac{\mathrm{d}S_t}{\mathrm{d}t} = 0$$

$$\text{or } S_t\frac{\mathrm{d}}{\mathrm{d}t}(S + C + E) + \varsigma_{a\theta}\frac{\mathrm{d}S_t}{\mathrm{d}t} = 0.$$

We noted that the first term was always larger than the second term within the stratosphere during the northern summer. Thus qualitative interpretation of the conservation of vorticity and potential vorticity thus carry similar messages from the mutual exchange of vorticity among S, C and E. Thus, there is present a measure for shear potential vorticity going into curvature potential vorticity under the constraints of conservation of PV. This to a first approximation is the same problem as that in the conservation of vorticity except for a multiplication factor which is the stability that varies somewhat more slowly.

The issue of diabatic heating is not a primary focus of this study. We have calculated the vertical flux of anticyclonic vorticity and of the conversion of shear vorticity to curvature vorticity on a daily basis. This is done from daily analysis fields that are already influenced by the heating.

The vorticity budget needs to be addressed in this context. All of the terms of the vorticity equation were calculated over the entire Northern Hemisphere for August 1988. The mean values for the vertical advection $-\omega\frac{\partial}{\partial p}\varsigma_a$ are illustrated in Figs. 13(a–c). These show the vertical layer averaged values of vertical advection for 10–100, 100–200 and 200–300 level. The most conspicuous features are the large negative values over the Tibetan Plateau and the Indian monsoon especially for the layers 10–100 and 100–200 hPa. These values are as large as -2^{-10} to -3^{-10}. These are regions of large upward flux of anticyclonic relative vorticity (since $\frac{\partial f}{\partial p} = 0$). This is consistent with the other findings of this study. The horizontal advection is large being of the order of -10^{-10}. This merely moves the vorticity from one location to another in the horizontal direction and was not of primary interest for the phenomena we are presenting here. The twisting terms were of the order of 10^{-13} to 10^{-14}. These were also the region where the largest conversion from anticyclonic shear to anticyclonic curvature was also noted.

Vertical motions vary from one re-analysis to another on a daily basis. However, we noted that, on monthly time scales, the NCEP and the ERA 40 do seem to show considerable agreement in the lower stratosphere and the upper troposphere. A month long time scale is relevant for our study since parcel trajectories

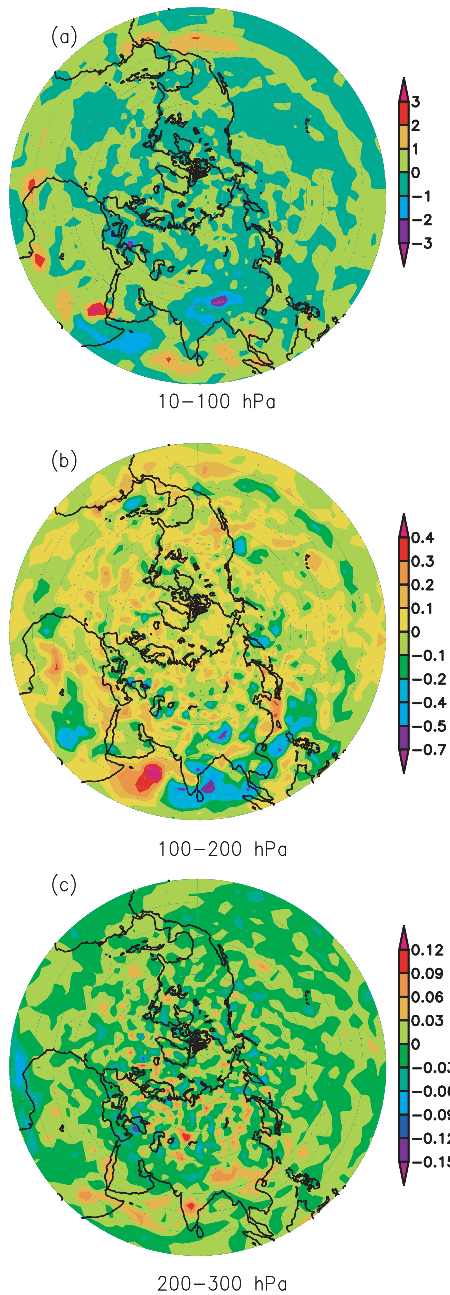

Fig. 13. Mean values of vertical advection (Pa s^{-2}) showing vertical averaged values for (a) 10–100 hPa levels (b) 100–200 hPa levels and (c) 200–300 hPa levels. Coastline is shown as solid line.

emanating from the monsoon upper troposphere take roughly 30 d to carve out a clockwise gyre around the pole at the 10 hPa level.

5. Conclusions and future work

In this paper, we have highlighted a clockwise anticyclonic gyre of circulation that extends up from the Asian monsoons (in the troposphere) to a polar circulation centred at the North Pole. This appears as a tilted cone of circulation that encircles the Northern Hemisphere at the 10 hPa level as we proceed down in the atmosphere, it almost tapers down to a point in the mid-troposphere of the monsoon region. The tropical easterly jet of the Northern Hemisphere resides near 10°N with its maximum winds near 35 m s^{-1} at the 175 hPa level. Most of the monsoonal heavy precipitation is located north of this jet where anticyclonic shear and anticyclonic curvature prevails. The upward motions of the summer monsoon carry parcels upward where a northern summer stratospheric fountain and a transport of large scale anticyclonic relative vorticity from the troposphere to lower stratosphere is a part of this scenario. We show that this lower stratosphere's kinematics carries a rich environment for the conversion of anticyclonic shear vorticity to the anticyclonic curvature vorticity. Swaths of four-dimensional parcel trajectories emanating from this stratospheric fountain carve out a hemispheric wide clockwise flow as this air rises to the 10 hPa level. This cone is an interesting connection between the North Polar anticyclone of the stratosphere at 10 hPa and the Asian summer monsoon. Vertical connection between pressure systems at different levels is normally done with hydrostatic reasoning. This is not based on reasoning from a simple hydrostatic vertical structure, here the aforementioned kinematics of flows appears important for the vertical connection of this tilted and massive system.

In this study, we identify a stratospheric fountain of anticyclonic vorticity during northern hemispheric summer over the Asian monsoon region emanating from the upper troposphere into the stratosphere where the kinematics of anticyclonic shear to curvature contributes to the production and maintenance of a near hemispheric anticyclonic flow over the Polar Regions of the stratosphere. It is clearly seen that the anticyclonic shear vorticity, seen to the north of the tropical easterly jet in the upper troposphere is transported upward to the lower stratosphere, and is steadily converted to anticyclonic curvature vorticity as the air parcels trajectories undergo a clockwise rotation. The associated near hemispherical horizontal extension and northward shift of the ridge, as we proceed from upper troposphere to the stratosphere, is facilitated by the kinematics of the conversion of the anticyclonic shear flow vorticity to anticyclonic shear flow vorticity. This suggests the maintenance of the anticyclonic flows of the stratosphere from the tropospheric Asian monsoon complex.

Our future study will extend this work. We have noted a quasi-biennial oscillation in the size of this cone. That is in fact related to the alternation of westerly and easterly winds over the equatorial latitudes, that is, the QBO near the 10 hPa levels. The roots of this phenomenon seem to lie in the tropospheric biennial oscillations (TBO) of the monsoon and SST anomalies of the Bay of Bengal and the Western Pacific ocean on the same time scales.

6. Acknowledgments

The research reported here was supported by the following grants: NSF ATM-0419618 and NOAA ARC-NA16GP1365. ECMWF ERA-40 data used in this study have been obtained from the ECMWF data server. Thanks are due to Dr. Arindam Chakraborty for editorial assistantship for the manuscript. Thanks are due to the two anonymous reviewers for their critical review and suggestions.

References

Atticks, M. G. and Robinson, G. D. 1983. Some features of the structure of the tropical tropopause. *Q. J. R. Met. Soc.* **109**, 295–308.

Bell, G. D. and Keyser, D. 1993. Shear and curvature vorticity and potential-vorticity interchanges: interpretation and application to a cutoff cyclone event. *Mon. Wea. Rev.* **121**, 76–102.

Chen, T. C. 2005. Maintenance of the mid-tropospheric North African summer circulation: Saharan high and African easterly jet. *J. Clim.* **18**, 2943–2962.

Danielsen, E. F. 1993. In situ evidence of rapid, vertical, irreversible transport of lower tropospheric air into the lower tropical stratosphere by convective cloud turrets and by larger-scale upwelling in tropical cyclones. *J. Geophys. Res.* **98**, 8665–8681.

Frederick, J. E. and Douglass, A. R. 1983. Atmospheric temperatures near the tropical tropopause: temporal variations, zonal asymmetry and implications for stratospheric water vapor. *Mon. Wea. Rev.* **111**, 1397–1403.

Gibson J. K., Kållberg, P., Uppala, S., Hernandez, A., Nomura, A., and co-authors. 1997. ERA description. ERA-40 Project Report Series 1, ECMWF, Reading, UK .

Hastenrath, S. 1991. *Climate Dynamics of the Tropics*. Kluwer Academic Publishers, Dordrecht, The Netherlands , 488 pp.

Kalnay, E., Kanamitsu, M., Kistler, R., Collins, W., Deaven, D., and co-authors. 1996. The NCEP/NCAR 40-year reanalysis project. *Bull. Amer. Met. Soc.* **77**, 437–471.

Koteswaram, P. 1958. The easterly jet stream in the tropics. *Tellus* **10**, 43–57.

Krishnamurti, T. N. and Bhalme, H. N. 1976. Oscillations of a monsoon system. Part I. Observational aspects. *J. Atmos. Sci.* **33**, 1937–1954.

Krishnamurti, T. N. and Bounoua L. 1996. *An Introduction to Numerical Weather Prediction Techniques*. CRC Press Inc., USA.

Mote, P. W., Rosenlof, K. H., McIntyre, M. E., Carr, E. S., Gille, J. C., and co-authors. 1996. An atmospheric tape recorder: the imprint of tropical tropopause temperatures on stratospheric water vapor. *J. Geophys. Res.* **101**(D2), 3989–4006.

Newell, R. E. and Gould-Stewart, S. 1981. A stratospheric fountain? *J. Atmos. Sci.* **38**, 2789–2796.

Parthasarathy, B., Munot, A. A. and Kothawale, D. R. 1995. Monthly and seasonal rainfall series for All-India homogeneous regions and meteorological subdivisions: 1871–1994. Contributions from the Indian Institute of Tropical Meteorology. Research Report RR-065, Aug. 1995.

Rao, Y. P. 1976. Southwest monsoon. *Meteorological Monograph (Synoptic Meteorology), No.1/1976*, India Meteorological Department, New Delhi , 366 pp.

Viudez, A. and Haney, R. L. 1996. On the shear and curvature vorticity equations. *J. Atmos. Sci.* **53**, 3384–3394.